FAST CURRENT RAMP EXPERIMENTS ON TFTR

By

E.D. Fredrickson, K. McGuire, R.J. Goldston, M. Bell, B. Grek,
D. Johnson, A.W. Morris, F.J. Stauffer, G. Taylor, and M.C. Zarnstorff

MAY 1987

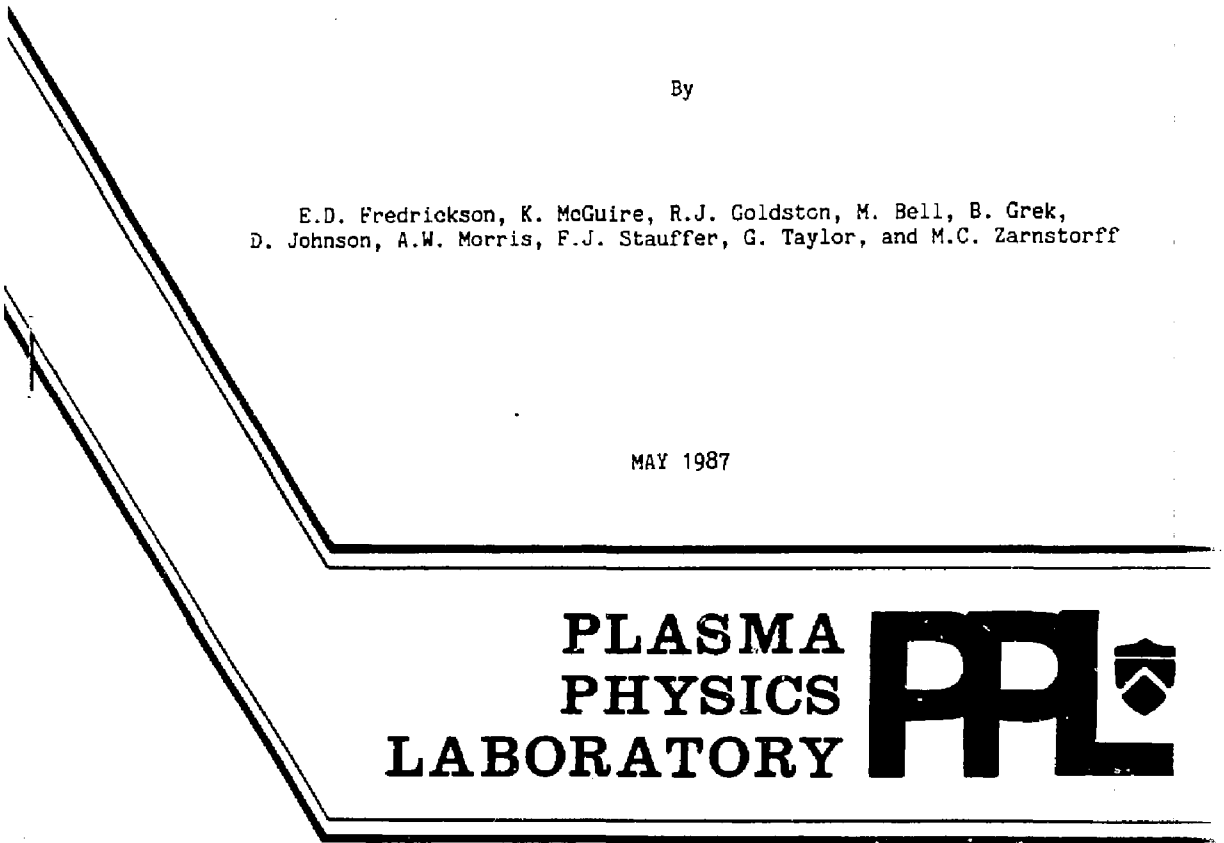

PRINCETON UNIVERSITY
PRINCETON, NEW JERSEY

PREPARED FOR THE U.S. DEPARTMENT OF ENERGY,
UNDER CONTRACT DE-AC02-76-CHO-3073.

Printed in the United States of America

Available from:

National Technical Information Service
U.S. Department of Commerce
5285 Port Royal Road
Springfield, Virginia 22161

Price Printed Copy $ * ; Microfiche $4.50

*Pages	NTIS Selling Price
1-25	$7.00
25-50	$8.50
51-75	$10.00
76-100	$11.50
101-125	$13.00
126-150	$14.50
151-175	$16.00
176-200	$17.50
201-225	$19.00
226-250	$20.50
251-275	$22.00
276-300	$23.50
301-325	$25.00
326-350	$26.50
351-375	$28.00
376-400	$29.50
401-425	$31.00
426-450	$32.50
451-475	$34.00
476-500	$35.50
500-525	$37.00
526-550	$38.50
551-575	$40.00
567-600	$41.50

For documents over 600 pages, add $1.50 for each additional 25-page increment.

PPPL--2437

DE87 013207

Fast Current Ramp Experiments on TFTR

E. D. Fredrickson, K. McGuire, R. J. Goldston
M. Bell, B. Grek, D. Johnson, A. W. Morris[†],
F. J. Stauffer[‡], G. Taylor, and M. C. Zarnstorff

Princeton Plasma Physics Laboratory
Princeton, NJ 08544

Abstract

Electron heat transport on TFTR and other tokamaks is several orders of magnitude larger than neoclassical calculations would predict. Despite considerable effort, there is still no clear theoretical understanding of this anomalous transport. The electron temperature profile, $T_e(r)$, shape has shown a marked consistency on many machines, including TFTR, for a wide range of plasma parameters and heating profiles. This could be an important clue as to the process responsible for this enhanced thermal transport. In this paper we describe what is meant by 'profile consistency' in TFTR and then discuss an experiment which uses a fast current ramp to transiently decouple the current density profile $J(r)$, and the $T_e(r)$ profiles. From this experiment we can determine the influence of $J(r)$ on electron temperature profile consistency.

[†]Permanent address: Balliol College, University of Oxford, UK
[‡]Permanent address: University of Maryland, College Park, MD

1 Temperature Profile Consistency

Observations of the consistency of the electron temperature profile have been reported on many machines (TFTR, Alcator, ASDEX, JET, T-10 etc.) [1-10]. In investigations of profile consistency, the profile shapes have traditionally been quantified in terms of the profile peaking parameter, $T_e(0)/\langle T_e \rangle$. This peaking parameter was found to scale strongly with $q(a)$ [1,2]. The independence of the $T_e(r)$ profile shape on the density or density profile shape weakened arguments that pressure-driven electrostatic modes were responsible for $T_e(r)$ profile consistency. Instead, the strong dependence of the peaking parameter on $q(a)$, together with the strong coupling of $T_e(r)$ and $J(r)$ through the plasma conductivity, suggested that the current profile might have a role in the electron temperature profile consistency, either through tearing modes [11] or through microscopic instabilities [12]. The inherent difficulty of electron temperature profile measurements in tokamaks made testing of these ideas difficult.

However, it has been realized that much of the scaling of the profile peaking parameter is due to the presence of sawtooth oscillations [7,13]. This dependence of the profile peakedness on the presence of sawteeth has been experimentally observed on PLT, ASDEX, and TFTR. In low q discharges where the current profile has been decoupled from the electron temperature (either with LHCD as on Alcator [2], ASDEX [14], and PLT [15] or transiently with a current ramp as on TFTR) so that sawteeth are absent, the profiles become peaked. Further, in high $q(a)$ neutral beam heated discharges (supershots) with strong central convection due to NB particle deposition [5], the profiles broaden, becoming similar in shape to lower $q(a)$ discharges. While these results contradict the old versions of profile consistency and call into question the role of $J(r)$, they also form the basis for even stronger statements of $T_e(r)$ profile constancy.

The study of electron temperature profile shapes, available from the multipoint Thomson scattering, ECE radiometer, and Michelson interferometer diagnostics, on TFTR has supported initial impressions that profile shapes are indeed more constant than known constraints can account for [3-6]. The shape of the profile outside approximately $0.4a$ (outside the sawtooth reconnection region in low q discharges) is found to be nearly invariant over a wide range of density, edge q and neutral beam heating power. In some cases, the profiles are more consistent with the additional

restriction that $T_e > 1$ keV, e.g., the 0.8 MA ohmic discharges beyond $0.7a$.

In these studies, the profile shapes are obtained by first symmetrizing the raw electron temperature profiles to remove Shafranov shift corrections, and then normalizing to the electron temperature at the half radius. Normalizing at the half radius, rather than the center, avoids the confusion introduced by sawteeth and similar effects. The symmetrization is typically done with a 'slice and stack' method where the Shafranov shift is calculated by assuming the electron temperature is constant on a flux surface. The results from this method agree well with the Shafranov shift calculated from β, the calculated current profile and toroidal effects.

Taking the profile for high $q(a)$ ohmic discharges (with very small sawteeth) as the 'limit' profile (Fig. 1a), it is found that the profile shape can be approximately fitted with the function

$$T_e(r)/T_0 \approx (1 - 0.95r/a)^{2/3} e^{-4r/3a}.$$

This function will then be used as a reference shape, not necessarily unique. In discharges with large central heat loss, e.g., with sawteeth or strong convection due to beam injection, this 'limit' profile shape is flattened in the core. It is this process that Gaussian profile consistency attempted to model. At the lowest $q(a)$, i.e., with large sawteeth present, the profiles can be approximately fitted with the above function or a Gaussian, but at higher $q(a)$ the profiles clearly differ from the Gaussian form proposed by B. Coppi [12].

$$T_e(r)/T_0 = exp[-2q(a)r^2/3a^2].$$

The constancy of the temperature profile shape outside approximately $0.4a$ implies that the logarithmic derivative of the temperature in this region is also invariant. This may have some implications for theoretical attempts to understand the profile conserving mechanism.

In Fig. 1b, the electron temperature profile shapes from high $q(a)$ neutral beam heated discharges (co-injection) are compared to the limit profile shape. The error bars represent the shot to shot variation in the profile shapes for discharges with heating powers from 3.6 to 10.6 MW. The Ohmic profile is more peaked, but outside of about $a/3$ the profile shape is unchanged within the experimental accuracy of the $T_e(r)$ measurements (approx. 10%). Figure 1c shows profile shapes, averaged over three similar shots, for balanced NBI heated discharges (supershots). The strongly

peaked beam deposition profile results in large central convective losses [5,16] causing a flattened profile. The independence of the profile shape outside $a/3$ on $q(a)$ is seen in Fig. 1d where the average profile shape from three similar ohmic $q(a) = 2.8$ discharges is compared to the limit profile shape.

Further evidence that it is the sawteeth that are responsible for flattening $T_e(r)$ (not only in the Kadomtsev sense, but on a time average over many sawteeth) within the reconnection region is found during the initial current ramp. For a short period of time, as the current diffuses in, $q(0)$ will be greater than one. During this time the $T_e(r)$ profile is close to the ideal profile constancy shape, independent of $q(a)$; but when $q(0)$ drops below one, sawtoothing begins and the central portion of the $T_e(r)$ profile flattens (Fig. 2).

The recovery of a drastically perturbed $T_e(r)$ profile may be studied during the reheat phase following pellet injection. In Fig. 3 normalized $T_e(r)$ profiles, beginning just before the pellet is injected (pellet injection is at 2.02 seconds), are shown. At 2.03 seconds, the central electron temperature has dropped from approximately 3.5 keV to 0.8 keV, and the profile shape is no longer constant. But by 3.0 seconds, the central electron temperature has recovered to 2.4 keV and the shape outside of $0.4a$ is now the limit profile shape.

As illustrated by the above examples, an assumption of profile constancy describes accurately the shape of $T_e(r)$ outside of $r/a \approx 0.4$ for full size TFTR plasmas. These results are consistent with the idea that χ_e varies with the heating profile shape to keep the profile constant. However, detailed transport analysis is required to determine the strength of this constraint. These results would also suggest that in a specific discharge the temperature profile shape will resist changes expected from changes in the heating profile. This picture fits nicely with the observed discrepancy between the rate of the heat pulse propagation and the power balance analysis for χ_e[17]. The next section of this paper will discuss experiments in which transient perturbations were used to determine the role of the current profile in electron temperature profile consistency.

2 Current Profile Consistency

The observation of profile consistency, coupled with the observed degradation in energy confinement with auxiliary heating (which tends to modify the heating profile), suggests that the thermal diffusivity, χ_e, may be a strong function of the temperature profile. This could be a direct dependence of χ_e on the $T_e(r)$ profile, its derivative, or upon related quantities such as the current density, $J(r)$, or $q(r)$. For many tokamaks, these profiles are fairly strongly coupled, making determination of the dependence of χ_e on $T_e(r)$ or $J(r)$ or their derivatives difficult. However, in TFTR where the resistive time constant can be several seconds, $T_e(r)$ and the calculated $J(r)$ are not in equilibrium for one or two seconds following the beginning of the current flattop. It is interesting to note that the electron temperature reaches its 'profile consistent' shape before the plasma current profile reaches resistive equilibrium. Figure 2 shows three electron temperature profiles measured during the initial current ramp. The discharge begins sawtoothing at about 1.4 seconds, modifying the central profile shape, but the profiles outside of $r/a \approx 0.4$ are remarkably invariant. Analysis of these discharges has provided useful information on the role of $J(r)$ in profile consistency. Experiments done with fast current ramps have even more strongly, if transiently, decoupled the $J(r)$ and $T_e(r)$ profiles.

As most inferred current profiles on TFTR are stable or marginally stable to low m tearing modes, tearing mode induced transport has been suggested as a possible explanation for the observed consistency of the $T_e(r)$ profile. The hypothesis is that tearing mode stability can depend sensitively on the current profile shape; thus, modes should grow quickly as a result of small perturbations to the $J(r)$ or $T_e(r)$ profiles, feeding back through enhanced local heat transport to keep $T_e(r)$ and hence $J(r)$ stable and, indirectly, consistent. The current ramp experiments offer the opportunity to test this hypothesis. The discharge was monitored for MHD activity during and following the ramp, and a code was developed to calculate the stability of TFTR current profiles to tearing modes.

Fast current ramps were done both with ohmic and neutral beam heated discharges. To avoid the problems inherent in analysis of the initial current ramp (e.g., unknown initial $J(r)$), a stable, low current plasma was established and allowed to equilibrate for approximately one second. In the first example (Fig. 4) the plasma current was ramped for 0.25 seconds at a rate

of 3.2 MA/sec to a final plasma current of 2.2 MA. The initial edge q was about 5.2 which then dropped to 3.3. While this ramp rate did not result in disruptions, bursts of MHD activity were observed during the ramp as the $q = 5, 4.5, 3$ rational surfaces passed through the edge of the plasma (Fig. 5).

In a second example (Fig. 6), the addition of 6 MW of neutral beam heating coincident with the current ramp resulted in slightly different MHD characteristics. Rather than the descending sequence of edge modes, internal $m/n = 2/1$ and $3/1$ modes were destabilized, along with the $m/n = 4/1$ mode when the $q = 4$ surface passed through the edge of the plasma (Fig. 7). Faster current ramps were not possible due to hardware limitations. Ramps at slower rates were not notably different, except for the absence of the bursts of MHD activity.

Since the purpose of this experiment was the study of plasmas in which $J(r)$ and $T_e(r)$ were not in equilibrium, the assumption of classical resistive current diffusion in the calculation of $J(r)$ must be examined. Previous experiments have suggested that the current diffusion can be anomalous at high ramp rates [18]. Measurements of the current profile shape are not available yet on TFTR, so for this work the current profiles were calculated with a time dependent current diffusion code [19]. These calculations predict the time dependent Λ ($\equiv \beta_{pol} + l_i/2$) and location of the $q = 1$ surface. These predictions can then be compared to the experimental measurements of these quantities as a check on the current diffusion simulation.

The time dependent Λ is sensitive to the gross current profile shape, but not to details of $J(r)$ in the core region. In the experiment, the measured Λ overshot the final value, dropping from about 0.9 to 0.55, below the typical value for a 2.2 MA plasma of 0.75. The Λ then recovered with a time constant of about 0.5 sec., reaching a value of 0.75 by the end of the discharge. This result is consistent with the classical resistive current penetration calculations which predict strong skin currents in the plasma edge (Fig. 8a). The location of the $q(r)1$ surface may be inferred from measurement of the sawtooth inversion radius. The time evolution of the $q(r)1$ surface measured in this way was in reasonable agreement with that calculated by the resistive current diffusion code (Fig. 8b). The offset is due to small uncertainties in the $T_e(r)$ profile.

A small edge disruption was observed, coincident with the passage of the $q = 4$ surface through the edge of the plasma. This disruption was

seen experimentally as a short increase in Λ, the presence of an $m/n = 4/1$ oscillation, and the loss of edge plasma temperature. The $m/n = 4/1$ mode caused a rapid drop in the edge temperature: at $r = 70cm$ (approximately $12cm$ from the limiter) the electron temperature dropped from 500 to 100 eV. This high resistivity region allowed the skin current to diffuse rapidly causing a short increase both in the Λ experimentally observed and in the current diffusion simulations. Thus the observed MHD activity did not cause measurable anomalous current penetration, but in this case did enhance the current diffusion by lowering the plasma temperature. Bursts of MHD activity were also observed at the passage of the $m/n = 5/1$ and $9/2$ rational surfaces through the plasma edge. These bursts were not observed to affect the current diffusion or plasma temperature. Thus in these discharges low m number tearing modes apparently affect current penetration through modification of the $T_e(r)$ profile.

The calculated current profiles were also tested for theoretical tearing mode stability with a $\Delta'_{m,n}$ code. The code solves the equation

$$(\partial^2/\partial r^2 + 1/r\partial/\partial r)\tilde{\psi} = (mqR_o/(rB_T(m - nq))(\partial J/\partial r)\tilde{\psi}$$

to get the perturbed helical flux function, $\tilde{\psi}(r)$, from which

$$\Delta'_{m,n} \equiv ((\partial\tilde{\psi}/\partial r)^+ - (\partial\tilde{\psi}/\partial r)^-)/\tilde{\psi}$$

is calculated [20]. Toroidal effects are included to the extent that $q(r)$ and $J(r)$ are mapped from the toroidal equilibrium code to radial coordinates. [The mapping is done by averaging the minor radius over the flux surface to map ψ to r and averaging $J(\psi, R)$ to get $J(\psi)$ and thus $J(r)$.] Pressure and D_R effects [21] are ignored in these calculations. Positive values of $\Delta'_{m,n}$ indicate instability and the island width, w, can be predicted by solving $\Delta'(w) = 0$ [22]. The stability calculations were done at each time point, giving the stability of each mode, $\Delta'_{m,n}(t)$, throughout the shot. The calculations were done for modes with $m/n > 1$ and in the range $6 \geq m \geq 2$.

Comparison of the $\Delta'_{m,n}$ calculations with the observed MHD activity during the current ramp in these two examples (Figs. 5 and 7) showed good agreement. The $\Delta'_{m,n}$ calculations accurately predicted the unstable edge tearing modes, even though this is where the shape of the current profiles is least well known. In addition, the calculations also predicted the instability of the $m/n = 2/1$ mode at the correct time, but the $m/n = 3/1$ mode was

calculated to be stable (Fig. 7). Other modes were calculated to be stable, even for the most strongly perturbed current profiles. These results are suggestive, but it is likely that the calculation of the current density profile is not sufficiently accurate (and the theory sufficiently incomplete) to make a detailed comparison meaningful at present.

Measurements of the electron temperature profile throughout the current ramp showed that the $T_e(r)$ profile shape remained relatively constant while the calculated $J(r)$ was strongly modified (Figs. 9a and 9b). The central T_e changed on the same time scale as the plasma current, i.e., about a half second. In the ohmic current ramp experiment, due to the large skin current, the ohmic heating power dissipated in the edge ($r \gtrsim 60cm$) increases by an order of magnitude. However, this results in a change in the total heat flux through the edge region of only about 50%. This change in the heating profile is too small to be useful in determining the dependence of transport on the heating profile. In the neutral beam heated cases, the change in the heat flux due to the change in ohmic heating profile was even less. Calculations of tearing mode stability showed that the current profile, although strongly modified, remained predominantly stable to tearing modes. This result was supported qualitatively with the Mirnov coil measurements. Further, while the 4/1 did strongly affect transport, the other modes had no measurable effect on the temperature profile or current diffusion. The conclusion is that low m tearing mode induced transport plays a minor role in maintaining electron temperature consistency.

3 Summary

In conclusion, the study of electron temperature profiles on TFTR has disproven some of the old ideas on profile consistency, and suggested a new form of profile constancy to take its place. Much of the old data on profile consistency can be explained by the effect of sawteeth on the electron temperature profile. The above analysis is consistent with a profile conserving mechanism which constrains the profile shape between the sawtoothing region and the plasma edge. More detailed radial transport analysis is required to determine how strongly χ_e responds to changes in the heating profile shape. The electron temperature profile shape outside $0.4a$ is found to be independent of the density and heating profile, as was the case before.

but, in addition, it is also independent of $q(a)$. A series of fast current ramp experiments were done to investigate the question of whether it is the $J(r)$ or $T_e(r)$ profile which is constrained. The results of this experiment shows that the $J(r)$ profile can be strongly modified, but that $T_e(r)$ is constant in the fashion described above.

Acknowledgments

The authors would like to thank H. P. Furth and A. Boozer for many helpful discussions. We would also like to thank the many TFTR physicists who provided so much of this excellent data. This work was supported by US DOE Contract No. DE-AC02-76CH03073.

References

[1] Taylor, G. et al., Nucl. Fusion 26 (1986) 339.

[2] Knowlton, S., in Proceedings of the Second Workshop on Transport and Profile Consistency in Tokamaks, University of Maryland, April 17-18, 1986 (unpublished).

[3] Fredrickson, E. et al., Controlled Fusion and Plasma Heating, 13th European Conference (1986) Vol. I, 148, Schliersee, F.R.G.

[4] Goldston, R. J. et al., Controlled Fusion and Plasma Heating, 13th European Conference (1986) Vol. I, 41, Schliersee, F.R.G.

[5] Goldston, R. J. et al., Kyoto 12th International Conference on Plasma Physics and Controlled Thermonuclear Fusion, Kyoto, IAEA-CN-47/A-II-1.

[6] Boyd, D. A., Kyoto 12th International Conference on Plasma Physics and Controlled Thermonuclear Fusion, Kyoto, IAEA-CN-47/AVI4.

[7] Goldston, R. J., Plasma Phys. Controlled Fusion 26 (1984) 87.

[8] Murman, H. et al., Controlled Fusion and Plasma Heating, 13th European Conference (1986) Vol. I, 216, Schliersee, F.R.G.

[9] Düchs, D. F. et al., 12th International Conference on Plasma Physics and Controlled Thermonuclear Fusion, Kyoto, IAEA-CN-47/A-VI-1-1.

[10] Esiptchuk, Yu. V. and Razumova, K. A., Plasma Phys. Controlled Fusion 28 (1986) 1253.

[11] Furth, H. P., Plasma Phys. Controlled Fusion 28 (1986) 1305.

[12] Coppi, B., and Tang, W., Princeton Plasma Physics Laboratory Report PPPL-2151.

[13] Waltz, R. et al., Nucl. Fusion 26 (1986) 1729.

[14] McCormick, K. et al., Controlled Fusion and Plasma Heating, 13th European Conference (1986) Vol. II, 323, Schliersee, F.R.G.

[15] Bernabei, S. et al., 12th International Conference on Plasma Physics and Controlled Thermonuclear Fusion, Kyoto, IAEA-CN-4/F-II-1.

[16] Strachan, J. et al., Phys. Rev. Lett. (to be published).

[17] Fredrickson, E. et al., Nucl. Fusion 26 (1986) 849.

[18] Stambaugh, R. et al., Nucl. Fusion 22 (1982) 395.

[19] Hawryluk, R. J., Phys. of Plasmas Close to Thermonuclear Ignition, Varenna 1979 (Vol. 1).

[20] Furth, H. P., Rutherford, P. H., and Selberg, H., Phys. Fluids 16 (1973) 1054 .

[21] Glasser, A. H., Greene, J. M., and Johnson, J. L., Phys. Fluids 19 (1976) 567 .

[22] White, R. B., Monticello, D., Rosenbluth, M. N., and Waddell, B. V., Phys. Fluids 20 (1977) 804 .

List of Figures

Figure 1a. The solid curve is the average of two normalized electron temperature profiles from ohmic high $q(a)$ discharges. The profiles have been mapped to flux surfaces to correct for the Shafranov shift. The dashed curve is a fitting function which approximates the $T_e(r)$ profile shapes for TFTR large major radius discharges (22022,22024). The dotted line is the old profile consistency shape, $T_e(r)/T_e(0) = \exp(2q_a r^2)/(3a^2)$, for $q(a) = 7$. ($q_{cyl}(a) \approx 7$, $< n_e > \approx 0.8 - 1.0 \times 10^{19}/m^3$, $I_p = 0.8MA$, $B_T = 4.5T$, and $T_e(0) \approx 3.6 - 4.2keV$.)

Figure 1b. The average of the normalized profiles from five neutral beam heated discharges with injected powers from 3.8 to 10.5 MW, again compared to an approximate limit profile shape (24001-24004,24006) ($q_{cyl}(a) \approx 7.7$, $< n_e >= 1.1 - 1.8 \times 10^{19}/m^3$, $I_p = 0.8MA$, $B_T = 4.8T$, $T_e(0) \approx 4 - 5keV$.)

Figure 1c. The average of profile shapes from three similar high $q(a)$ balanced NBI discharges ('supershots') (24280,24281,24282). ($q_{cyl}(a) \approx 7.8$, $< n_e >= 2.2 \times 10^{19}/m^3$, $I_p = 0.8MA$, $B_T = 4.8T$, $T_e(0) \approx 5.8keV$.)

Figure 1d. The average of profile shapes from three low $q(a)$ ohmic discharges (24088,24096,24909). ($q_{cyl}(a) \approx 2.9$, $< n_e >= 2.9 - 5.2 \times 10^{19}/m^3$, $I_p = 2.2MA$, $B_T = 4.8T$, $T_e(0) \approx 1.8 - 3.8keV$.)

Figure 2. Electron temperature profiles during the current ramp phase of a 2.2 MA plasma. The profiles are from 1.0, 1.5, and 2.0 seconds into the discharge. Sawteeth began at approximately 1.4 seconds and are presumably responsible for the change in profile shape. ($q_{cyl}(a) = 3.3$, 2.8, and 2.5 at 1.0, 1.5, and 2.0 seconds, respectively, from shot 12035.)

Figure 3. Normalized electron temperature profiles showing the $T_e(r)$ profile shape during the reheat following pellet injection. The times of the profiles are for 2.0 seconds, just before pellet injection, 2.03 seconds, just after injection, and at 3.0 and 3.5 seconds. The electron temperature dropped from 3.8 keV on axis at 2.0 seconds to 0.8 keV at 2.03 seconds with the pellet injection. (Shot 13640)

Figure 4. Current, density, temperature, and loop voltage for an ohmic current ramp shot. (Shot 17906)

Figure 5a. The envelope of MHD activity during the current ramp shot in Fig. 4. The bursts of MHD activity are identified by mode numbers

found from the phase analysis of the poloidal and toroidal array of Mirnov coils.

Figure 5b. The $\Delta'_{m,n}$'s calculated for the modes observed in Fig. 5a.

Figure 6. Current, density, temperature, and loop voltage for a current ramp shot with 6 MW of NB power. (shot 18741)

Figure 7a. The envelope of MHD activity seen during the neutral beam heated current ramp in Fig. 6. The MHD behavior is different than in the ohmic case of Fig. 4.

Figure 7b. The calculated $\Delta'_{m,n}$'s for the modes seen in Fig 7a. The agreement between experiment and calculation is not as good as in Fig. 5.

Figure 8a. Λ vs. time, calculated, and measured for the current ramp shot in Fig. 4.

Figure 8b. Approximate sawtooth inversion radius (dots) determined from the soft x-ray imaging system and the calculated q=1 surface for above assuming resistive, neoclassical current diffusion. The chord averaged inversion radii have been corrected by 1.3 to correct for chord averaging effects. Also plotted is $1/q(a)$, which is found to approximate the normalized inversion radius in equilibrium.

Figure 9a. Selected calculated current profiles from the NBI current ramp shot (Fig. 6). For most of the current ramp the $J(r)$ profile is hollow (although toroidal effects keep $q(r)$ monotonic in minor radius). The times for the profiles are: a - 2.5 sec., b - 2.7 sec., c - 3.0 sec., d - 3.5 sec., and e - 4.0 seconds.

Figure 9b. The normalized temperature profiles corresponding to the current profiles in Fig. 9a. Despite rather large changes in the current profile, the temperature profile shape remains invariant. The times for the profiles are as in Fig. 9a.

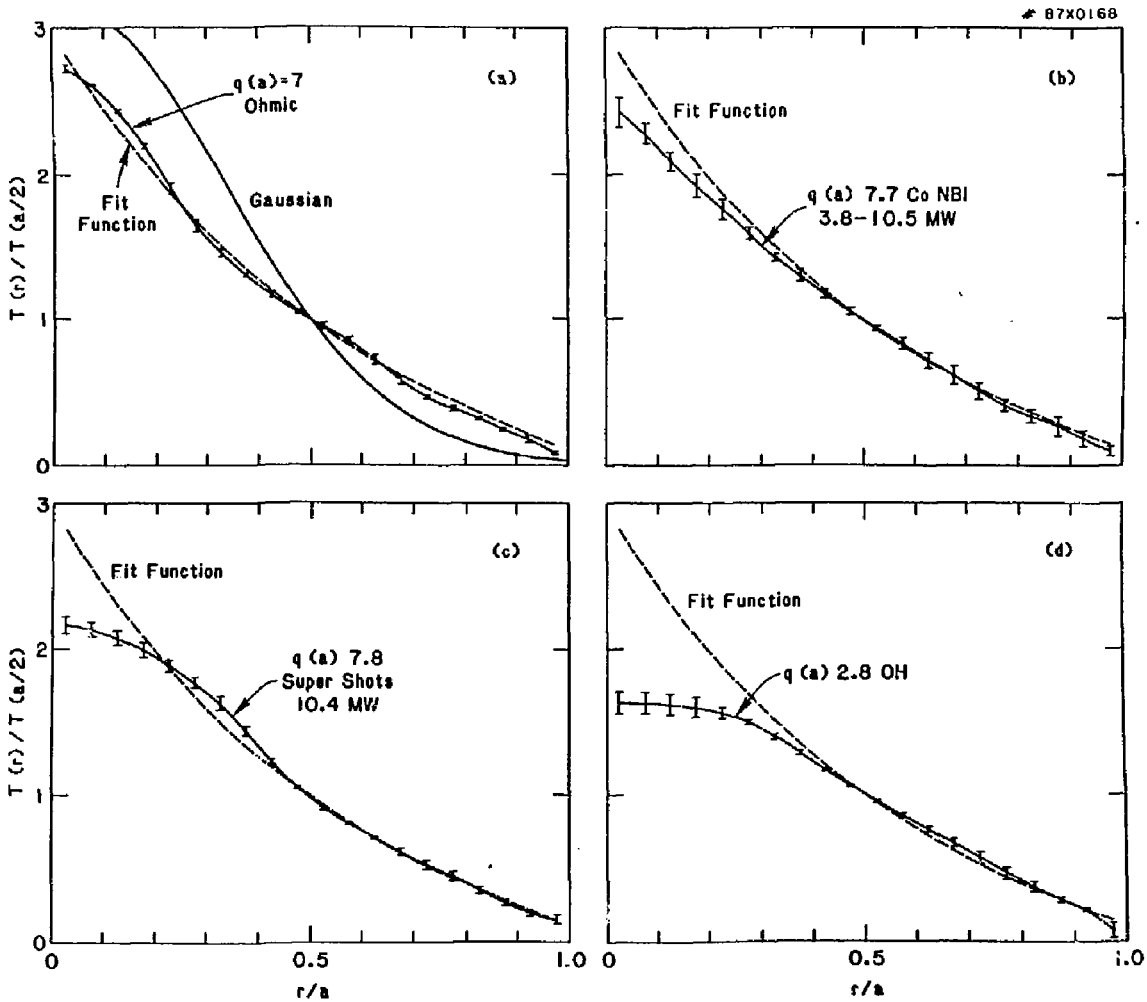
87X0168
(a)
q (a)=7
Ohmic
Fit
Function
Gaussian
(b)
Fit Function
q (a) 7.7 Co NBI
3.8-10.5 MW
(c)
Fit Function
q (a) 7.8
Super Shots
10.4 MW
(d)
Fit Function
q (a) 2.8 OH
T (r) / T (a/2)
r/a
0
0.5
1.0
1
2
3

Fig. 1 (a) - (d)

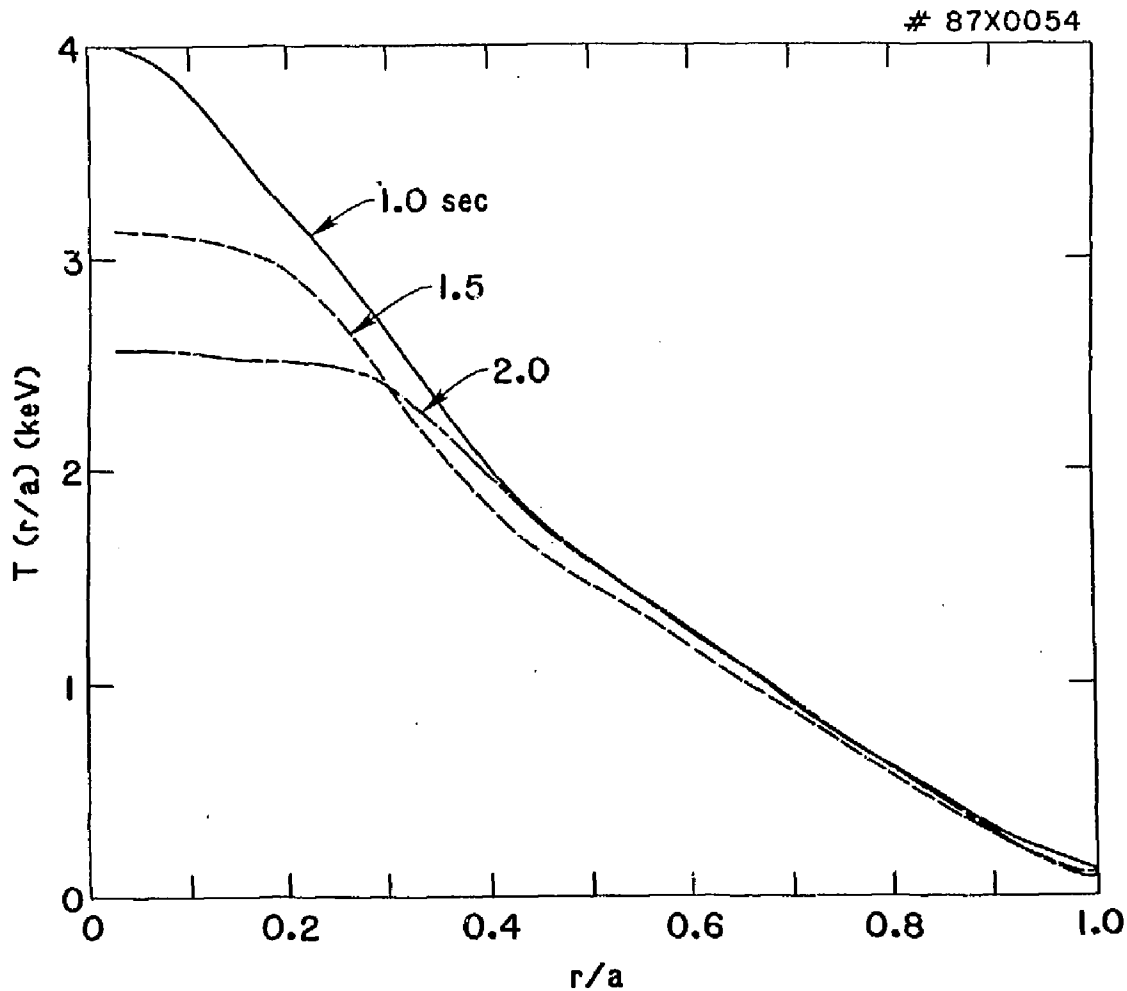

Fig. 2

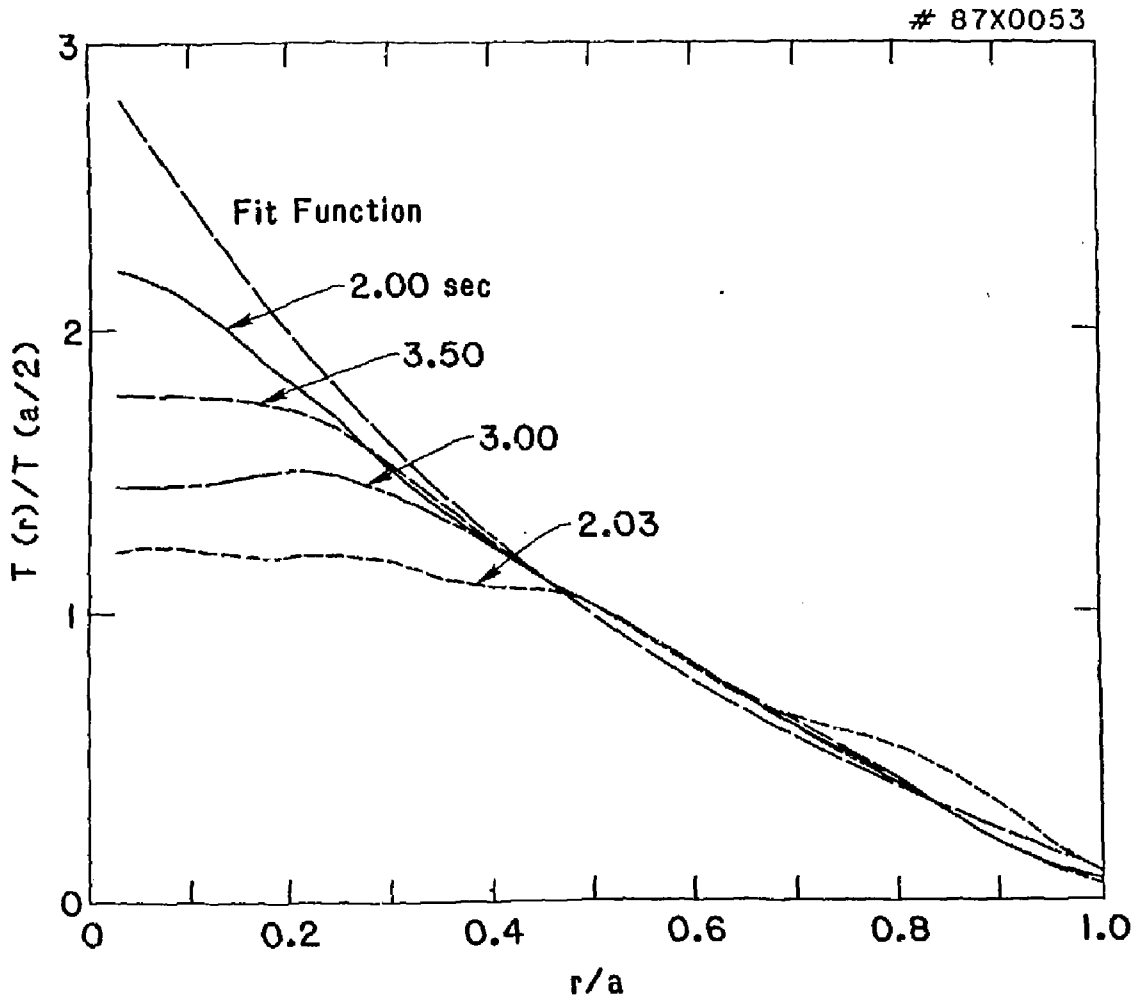
87X0053
Fit Function
2.00 sec
3.50
3.00
2.03
T (r)/T (a/2)
r/a
0
1
2
3
0
0.2
0.4
0.6
0.8
1.0

Fig. 3

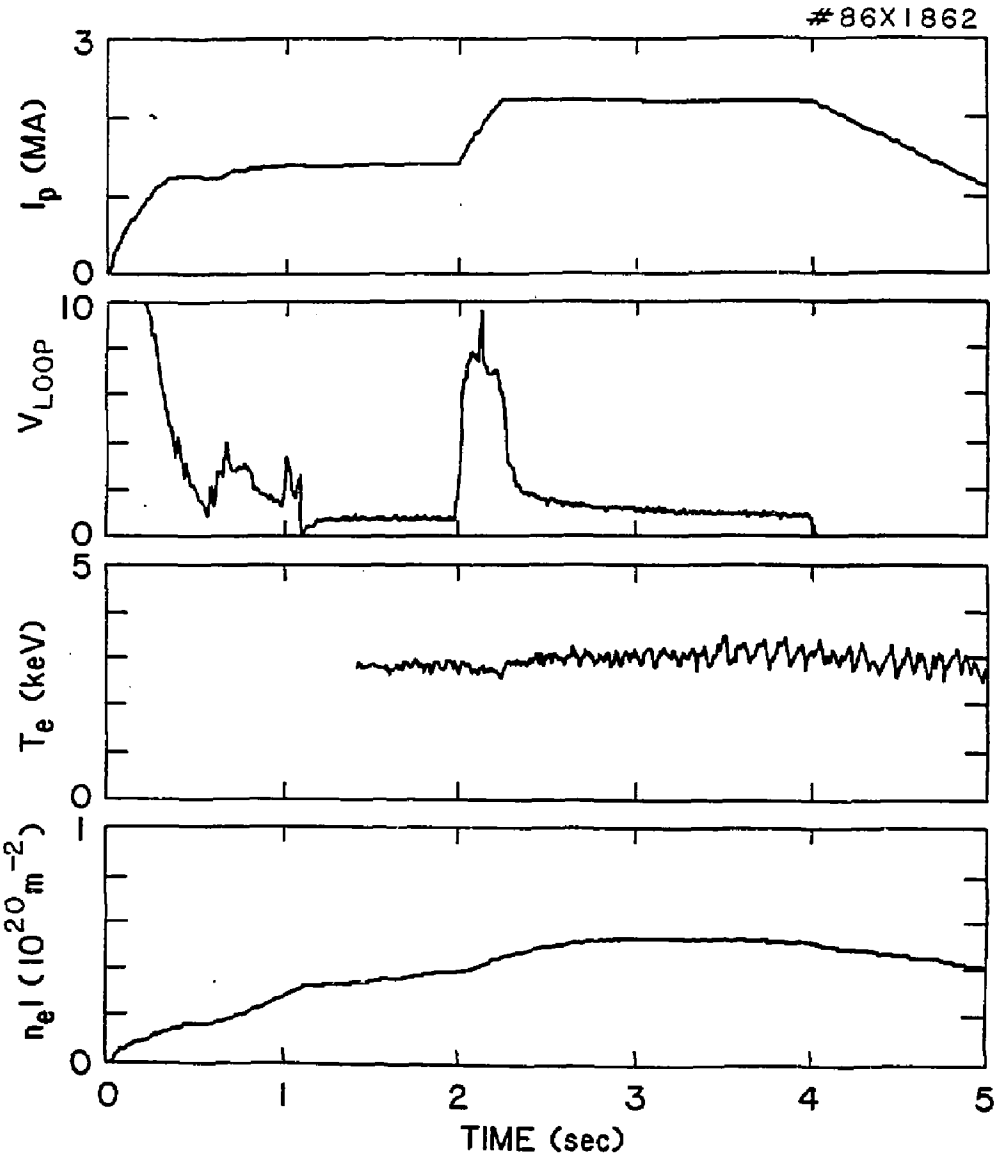
#86X1862
3
I_p (MA)
0
10
V_{LOOP}
0
5
T_e (keV)
0
1
$n_e l$ (10^{20} m^{-2})
0
0
1
2
3
4
5
TIME (sec)

Fig. 4

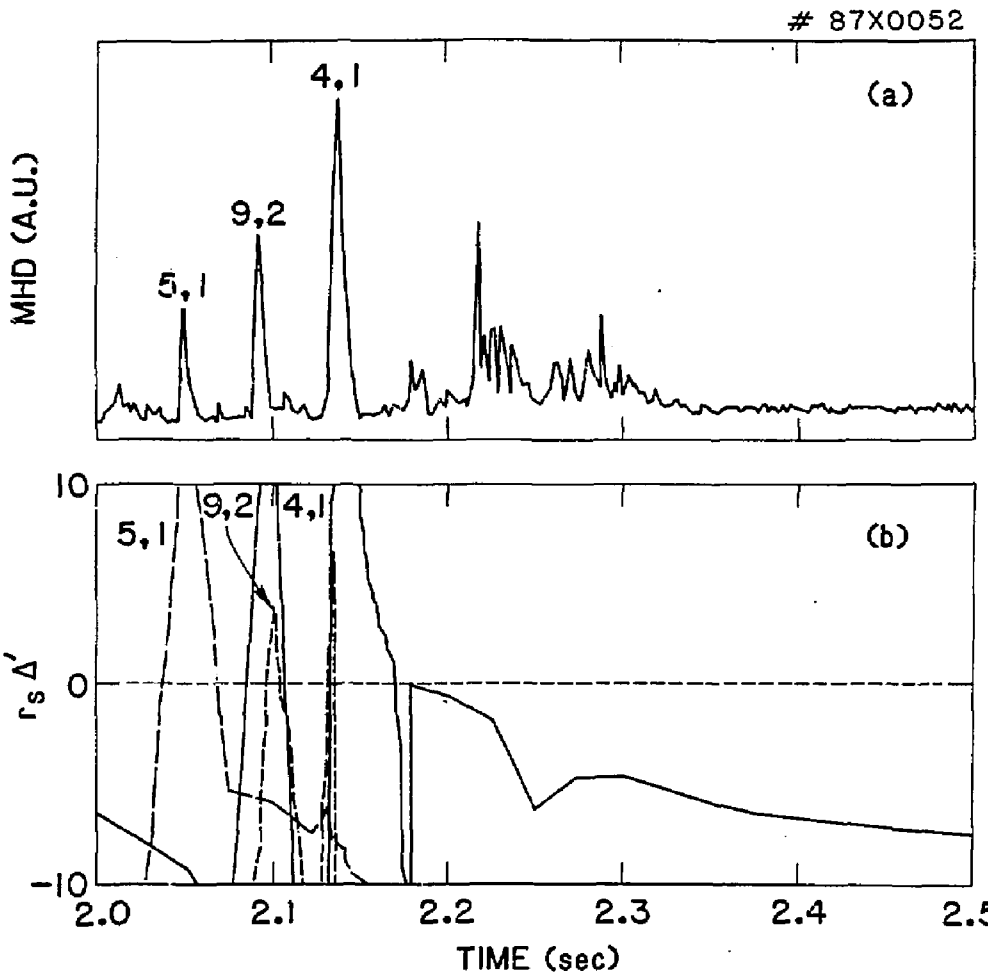
87X0052
(a)
MHD (A.U.)
4,1
9,2
5,1
(b)
$r_s\Delta'$
10
0
-10
2.0
2.1
2.2
2.3
2.4
2.5
TIME (sec)

Fig. 5 (a) - (b)

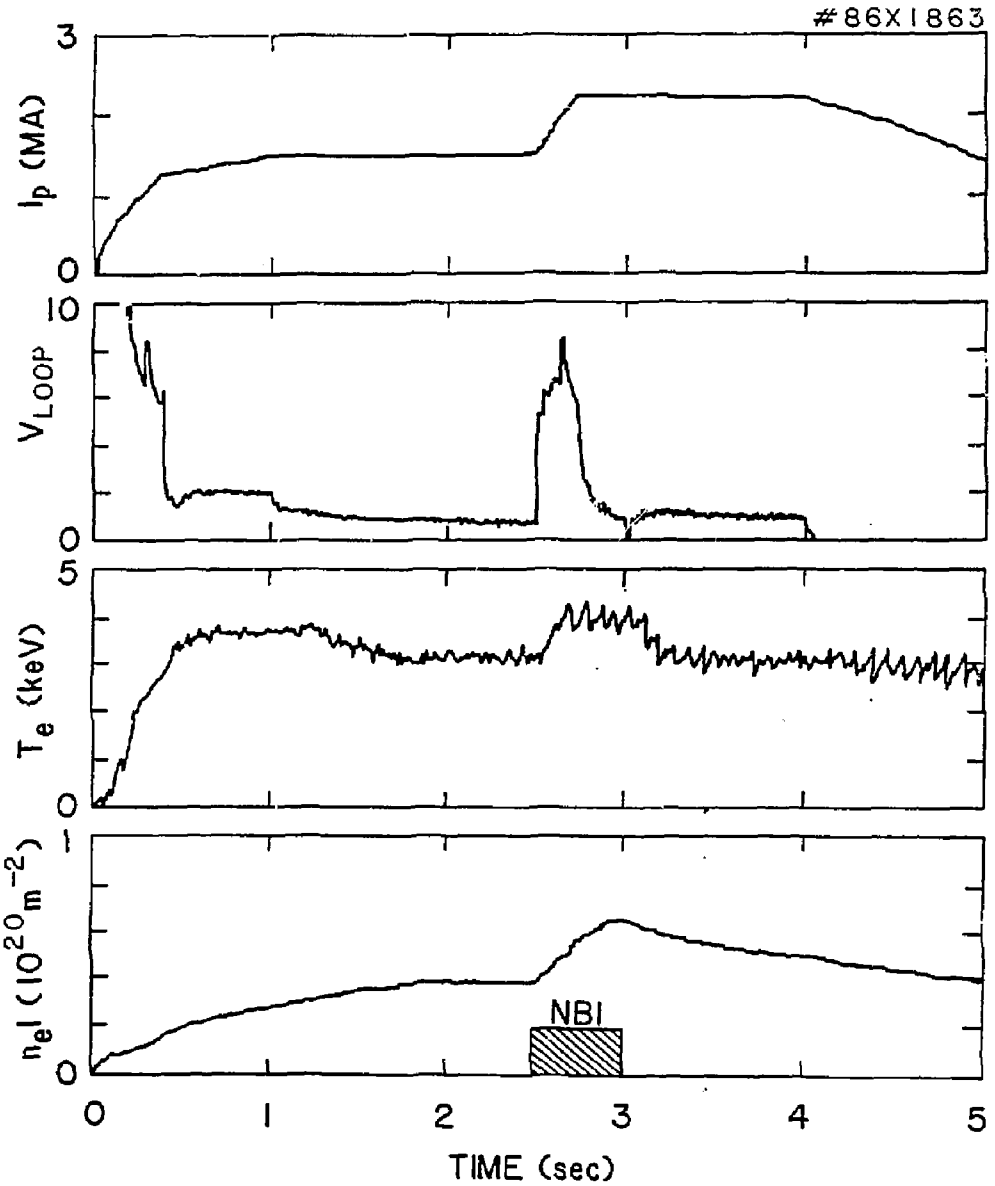
#86X1863
3
I_p (MA)
0
10
V_{LOOP}
0
5
T_e (keV)
0
$n_e l$ ($10^{20} m^{-2}$)
0
NBI
0
1
2
3
4
5
TIME (sec)

Fig. 6

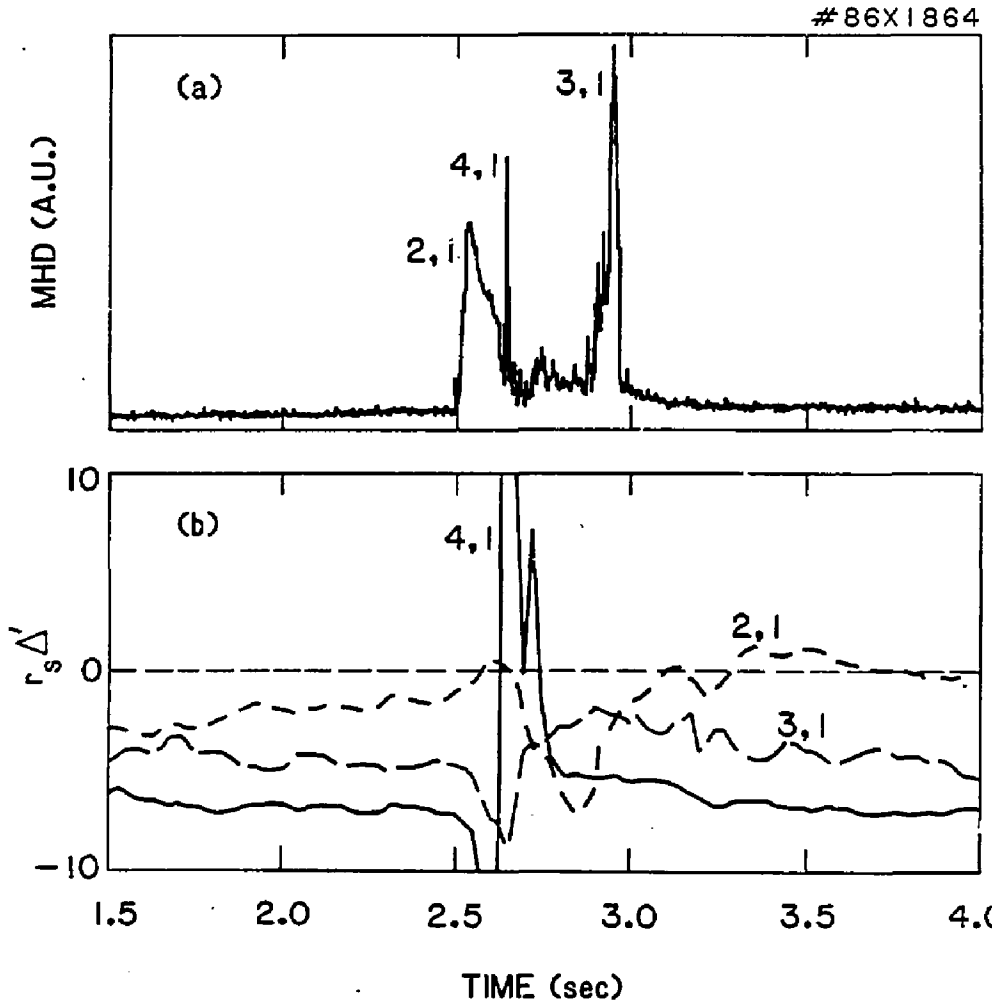
#86X1864
(a)
3,1
4,1
2,1
MHD (A.U.)
(b)
4,1
2,1
3,1
10
0
-10
$r_s\Delta'$
1.5
2.0
2.5
3.0
3.5
4.0
TIME (sec)

Fig. 7 (a) - (b)

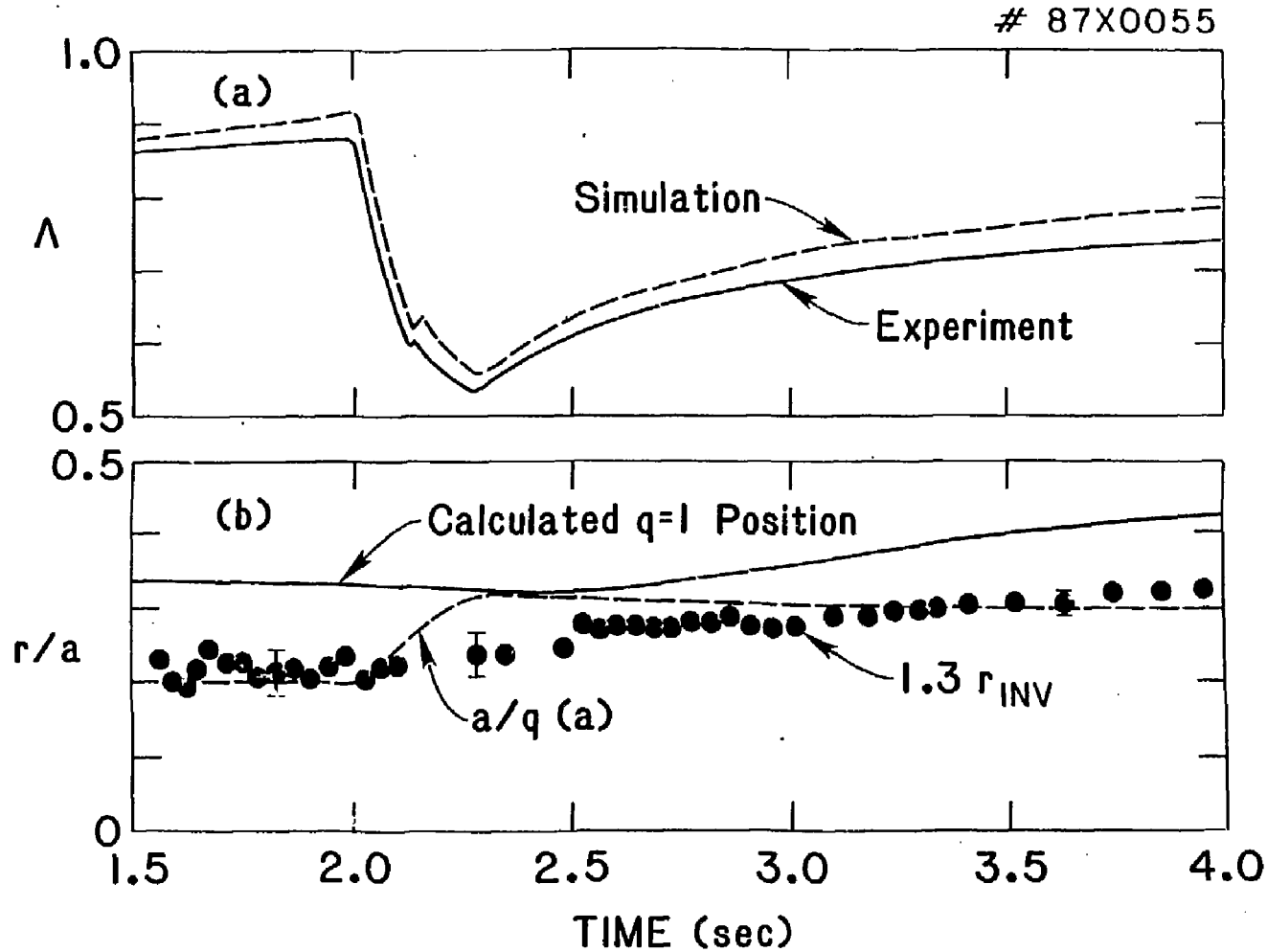
87X0055
1.0
(a)
Λ
Simulation
Experiment
0.5
0.5
(b)
Calculated q=1 Position
r/a
1.3 r INV
a/q (a)
0
1.5
2.0
2.5
3.0
3.5
4.0
TIME (sec)

Fig. 8 (a) - (b)

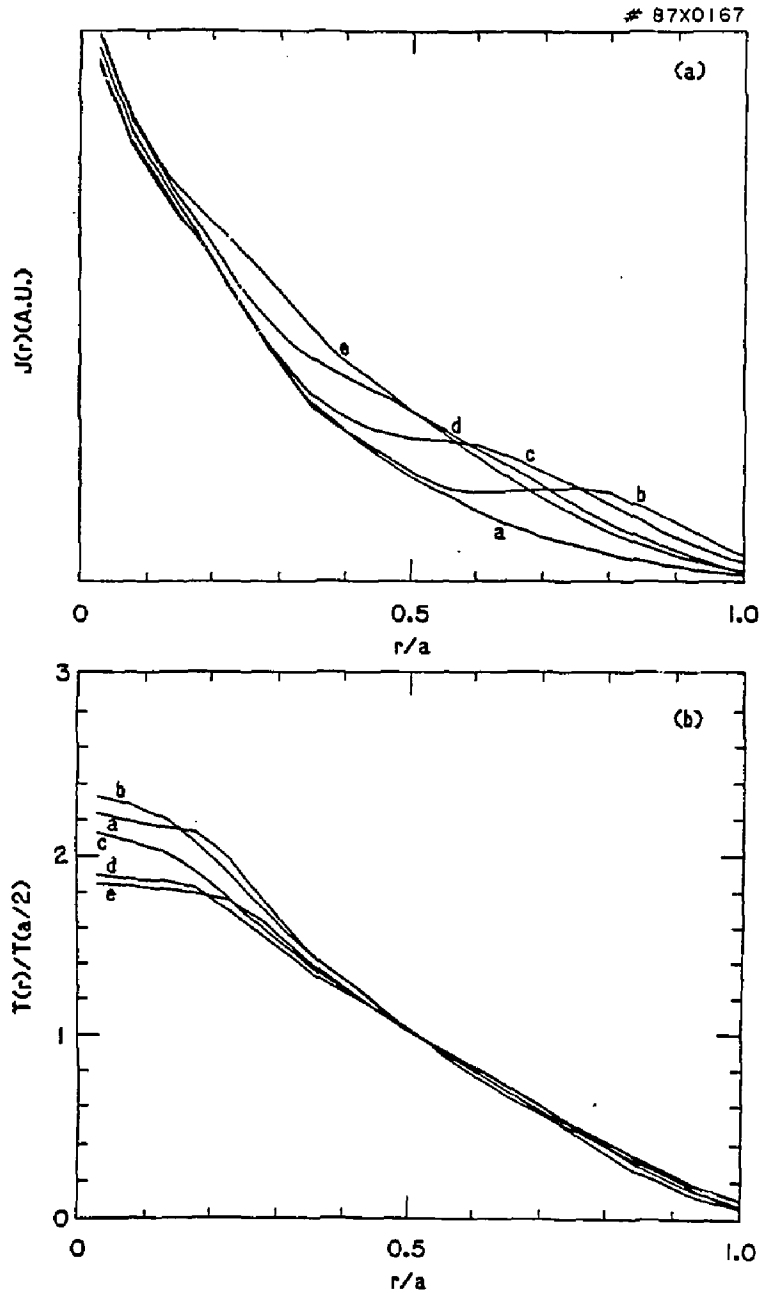

Fig. 9 (a) - (b)

EXTERNAL DISTRIBUTION IN ADDITION TO UC-20

Dr. Frank J. Paoloni, Univ of Wollongong, AUSTRALIA
Prof. M.H. Brennan, Univ Sydney, AUSTRALIA
Plasma Research Lab., Australian Nat. Univ., AUSTRALIA
Prof. I.R. Jones, Flinders Univ., AUSTRALIA
Prof. F. Cap, Inst Theo Phys, AUSTRIA
Prof. M. Heindler, Institut fur Theoretische Physik, AUSTRIA
M. Goossens, Astronomisch Instituut, BELGIUM
Ecole Royale Militaire, Lab de Phys Plasmas, BELGIUM
Com. of European, Dg XII Fusion Prog, BELGIUM
Prof. R. Boucique, Laboratorium voor Natuurkunde, BELGIUM
Dr. P.H. Sakanaka, Univ Estadual, BRAZIL
Instituto De Pesquisas Espaciais-INPE, BRAZIL
Library, Atomic Energy of Canada Limited, CANADA
Dr. M.P. Bachynski, MPB Technologies, Inc., CANADA
Dr. H.M. Skarsgard, Univ of Saskatchewan, CANADA
Dr. H. Barnard, University of British Columbia, CANADA
Prof. J. Teichmann, Univ. of Montreal, CANADA
Prof. S.R. Sreenivasan, University of Calgary, CANADA
Prof. Tudor W. Johnston, INRS-Energie, CANADA
Dr. C.R. James, Univ. of Alberta, CANADA
Dr. Peter Lukac, Komenskeho Univ, CZECHOSLOVAKIA
The Librarian, Culham Laboratory, ENGLAND
Mrs. S.A. Hutchinson, JET Library, ENGLAND
C. Mouttet, Lab. de Physique des Milieux Ionises, FRANCE
J. Radet, CEN/CADARACHE - Bat 506, FRANCE
Dr. Tom Mual, Academy Bibliographic, HONG KONG
Preprint Library, Cent Res Inst Phys, HUNGARY
Dr. B. Dasgupta, Saha Inst, INDIA
Dr. R.K. Chhajlani, Vikram Univ, INDIA
Dr. P. Kaw, Institute for Plasma Research, INDIA
Dr. Phillip Rosenau, Israel Inst Tech, ISRAEL
Prof. S. Cuperman, Tel Aviv University, ISRAEL
Librarian, Int'l Ctr Theo Phys, ITALY
Prof. G. Rostagni, Univ Di Padova, ITALY
Miss Clelia De Palo, Assoc EURATOM-ENEA, ITALY
Biblioteca, del CNR EURATOM, ITALY
Dr. H. Yamato, Toshiba Res & Dev, JAPAN
Prof. I. Kawakami, Atomic Energy Res. Institute, JAPAN
Prof. Kyoji Nishikawa, Univ of Hiroshima, JAPAN
Direc. Dept. Lg. Tokomak Res. JAERI, JAPAN
Prof. Satoshi Itoh, Kyushu University, JAPAN
Research Info Center, Nagoya University, JAPAN
Prof. S. Tanaka, Kyoto University, JAPAN
Library, Kyoto University, JAPAN
Prof. Nobuyuki Inoue, University of Tokyo, JAPAN
S. Mori, JAERI, JAPAN
M.H. Kim, Korea Advanced Energy Research Institute, KOREA
Prof. D.I. Choi, Adv. Inst Sci & Tech, KOREA
Prof. B.S. Liley, University of Waikato, NEW ZEALAND
Institute of Plasma Physics, PEOPLE'S REPUBLIC OF CHINA
Librarian, Institute of Phys., PEOPLE'S REPUBLIC OF CHINA
Library, Tsing Hua University, PEOPLE'S REPUBLIC OF CHINA
Z. Li, Southwest Inst. Physics, PEOPLE'S REPUBLIC OF CHINA
Prof. J.A.C. Cabral, Inst Superior Tecn, PORTUGAL
Dr. Octavian Petrus, AL I CUZA University, ROMANIA
Dr. Johan de Villiers, Plasma Physics, AEC, SO AFRICA
Prof. M.A. Hellberg, University of Natal, SO AFRICA
Fusion Div. Library, JEN, SPAIN
Dr. Lennart Stenflo, University of UMEA, SWEDEN
Library, Royal Inst Tech, SWEDEN
Prof. Hans Wilhelmson, Chalmers Univ Tech, SWEDEN
Centre Phys des Plasmas, Ecole Polytech Fed, SWITZERLAND
Bibliotheek, Fom-Inst Voor Plasma-Fysica, THE NETHERLANDS
Dr. O.D. Ryutov, Siberian Acad Sci, USSR
Dr. G.A. Eliseev, Kurchatov Institute, USSR
Dr. V.A. Glukhikh, Inst Electro-Physical, USSR
Dr. V.T. Tolok, Inst. Phys. Tech. USSR
Dr. L.M. Kovrizhnykh, Institute Gen. Physics, USSR
Prof. T.J.M. Boyd, Univ College N Wales, WALES
Nuclear Res. Establishment, Julich Ltd., W. GERMANY
Bibliothek, Inst. Fur Plasmaforschung, W. GERMANY
Dr. K. Schindler, Ruhr Universitat, W. GERMANY
ASDEX Reading Rm, IPP/Max-Planck-Institut fur Plasmaphysik, W. GERMANY
Librarian, Max-Planck Institut, W. GERMANY
Prof. R.K. Janev, Inst Phys, YUGOSLAVIA